REGULAR ARTICLE

blood advances

Nurselike cells sequester B cells in disorganized lymph nodes in chronic lymphocytic leukemia via alternative production of CCL21

Rim Zaaboub,[1,2] Lene Vimeux,[3] Vincent Contremoulins,[4] Florence Cymbalista,[1,2,5] Vincent Lévy,[2,6,7] Emmanuel Donnadieu,[3] Nadine Varin-Blank,[1,2] Antoine Martin,[1,2,8,*] and Elisabetta Dondi[1,2,*]

[1]U978 Institut National de la Santé et de la Recherche Médicale, Bobigny, France; [2]Université Sorbonne Paris Nord, Alliance Sorbonne Paris Cité, Labex Inflamex, Bobigny, France; [3]Université Paris Cité, Centre National De La Recherche Scientifique (CNRS), INSERM, Equipe Labellisée Ligue Contre le Cancer, Institut Cochin, Paris, France; [4]Université Paris Cité, CNRS, Institut Jacques Monod, Paris, France; [5]Service d'Hématologie Biologique, Hopital Avicenne, Bobigny, France; [6]Département de Recherche Clinique, Hôpital Avicenne, Bobigny, France; [7]Centre de Recherche Epidemiologique et Statistique Unité Mixte de Recherche 1153 Epidemiology and Clinical Statistics for Tumor, Respiratory, and Resuscitation Assessments team, Hôpital Saint Louis, Paris, France; and [8]Service d'Anatomie Pathologique, Hôpital Avicenne, Assistance Publique – Hôpitaux de Paris, Bobigny, France

Key Points

- Stromal cell architecture is deeply altered in CLL lymph nodes.
- CCL21, produced by leukemia-induced macrophages, improves retention and niching of malignant CCR7$^+$ B cells in CLL lymph nodes.

Tumor microenvironment exerts a critical role in sustaining homing, retention, and survival of chronic lymphocytic leukemia (CLL) cells in secondary lymphoid organs. Such conditions foster immune surveillance escape and resistance to therapies. The physiological microenvironment is rendered tumor permissive by an interplay of chemokines, chemokine receptors, and adhesion molecules as well as by direct interactions between malignant lymphocytes and stromal cells, T cells, and specialized macrophages referred to as nurselike cells (NLCs). To characterize this complex interplay, we investigated the altered architecture on CLL lymph nodes biopsies and observed a dramatic loss of tissue subcompartments and stromal cell networks as compared with nonmalignant lymph nodes. A supplemental high density of CD68$^+$ cells expressing the homeostatic chemokine CCL21 was randomly distributed. Using an imaging flow cytometry approach, CCL21 mRNA and the corresponding protein were observed in single CD68$^+$ NLCs differentiated in vitro from CLL peripheral blood mononuclear cells. The chemokine was sequestered at the NLC membrane, helping capture of CCR7-high-expressing CLL B cells. Inhibiting the CCL21/CCR7 interaction by blocking antibodies or using therapeutic ibrutinib altered the adhesion of leukemic cells. Our results indicate NLCs as providers of an alternative source of CCL21, taking over the physiological task of follicular reticular cells, whose network is deeply altered in CLL lymph nodes. By retaining malignant B cells, CCL21 provides a protective environment for their niching and survival, thus allowing tumor evasion and resistance to treatment. These findings argue for a specific targeting or reeducation of NLCs as a new immunotherapy strategy for this disease.

Introduction

The tumor microenvironment plays an essential role in neoplasm progression through continuous molecular crosstalk and cellular interactions with tumor cells. Notably, this microenvironment is critical for tumor cell survival through the creation of a site of retention in favor of a proliferative pool. In turn,

Submitted 4 October 2021; accepted 31 May 2022; prepublished online on *Blood Advances* First Edition 9 June 2022; final version published online 12 August 2022. DOI 10.1182/bloodadvances.2021006169.

*A.M. and E.Dondi are joint senior authors.

Contact the corresponding author for data sharing: elisabetta.dondi@inserm.fr.

The full-text version of this article contains a data supplement.

this niching fosters immune survey escape and development of resistance to treatments. Chronic lymphocytic leukemia (CLL) is a mature B cell–derived neoplasm characterized by an accumulation of $CD5^+$ leukemic cells in the blood, bone marrow (BM), and secondary lymphoid organs.[1] New therapeutic options include kinase inhibitors, such as Bruton tyrosine kinase (BTK) inhibitor ibrutinib, that foster lymph node egress and release of leukemic cells. Besides several intrinsic mutational events at risk of progression and relapse in CLL, the tumor microenvironment clearly contributes to disease evolution and resistance to therapeutic regimen.[2,3] In lymphoid organs, the CLL microenvironment is shaped by a complex interplay among chemokines, their cognate receptors, and adhesion molecules as well as direct interactions of malignant B cells with $CD4^+$ and $CD8^+$ T cells, natural killer T cells, and specialized $CD68^+$ macrophages often referred to as tumor-associated macrophages (TAMs) or nurselike cells (NLCs).[4] NLCs are cells of monocytic origin and spontaneously differentiate in vitro in high-density cultures of CLL peripheral blood mononuclear cells (PBMCs). Importantly, NLCs have been described in lymphoid organs from patients with CLL.[5] Such NLCs prevent CLL cells from apoptosis in vitro, notably through the expression of BAFF or APRIL,[6] CD31, plexin-B1,[7] brain-derived neurotrophic factor,[8] and the secretion of soluble CXCL12.[9] Notably, CXCL12 behaves as an important player in the recirculation of plasma cells in BM niches[10,11] as well as in the *trans*-endothelial migration of CLL cells[12] and their homing to the BM.[13] In addition, NLCs secrete CXCL13, a homeostatic chemokine normally expressed by follicular dendritic cells (FDCs). CXCL13 interacting with its cognate receptor CXCR5 is responsible for lymphocytes homing in secondary lymphoid organs and active trafficking within follicles.[14] Leukemic cells express high levels of functional CXCR5, and significantly increased CXCL13 serum levels were described in patients with CLL compared with healthy controls. CXCL13 expressed by NLCs plays an important role in CLL cells niching. Cognate interactions of the leukemic cells with $CD68^+$ NLCs secreting CXCL13 allow CLL cells to receive prosurvival signals and partial protection against cytotoxic therapies.[15,16] The crosstalk between leukemic cells and their microenvironment also facilitates activation, proliferation, and differentiation of the surrounding cells, events that are essential to the transmission of supportive signals. In the context of this bidirectional crosstalk, NLCs are reprogrammed by leukemic cells to create an immunosuppressive milieu that allows immune evasion.

Additional factors play a role in the positioning of CLL cells within lymphoid subcompartments. Among those, the homeostatic chemokine CCL21, expressed by high endothelial venules (HEVs) and follicular reticular cells in the T-cell zone (FRCs), plays a pivotal role in driving cell entry and motility in interstitial lymph nodes, favoring their interaction with $CD4^+$ T cells expressing CD40L.[17] Knockout mice lacking the CCL21 cognate receptor CCR7 display defective B-cell entry into the lymph nodes.[18] In the Eμ-Myc transgenic mouse model, CCR7 was shown to play a pivotal role in several consecutive steps of leukemic cell dissemination within distinct microanatomic sites of the spleen, leading to a significant survival advantage of tumor cells compared with CCR7-deficient lymphoma cells.[19] Accordingly, *trans*-endothelial cell migration in response to CCL21 significantly increased for malignant B cells in patients who presented with lymph node enlargement. Furthermore, the level of expression of CCR7 correlated with lymphadenopathy, and its blockade inhibited CLL *trans*-endothelial cell migration.[20]

In CLL, the physiological architecture of the lymph nodes is completely obliterated by dissemination of malignant cells, which contributes to the immune surveillance defect commonly associated with disease progression. In this context, infiltrated NLCs may represent an alternative source of homeostatic chemokines taking over the roles attributed to FDCs and FRCs.

In this study, we addressed alteration of cellular structures in CLL lymph nodes, showing loss of subcompartments and stromal cell networks while exhibiting a high density of $CD68^+$ cells. Importantly, our data document for the first time that $CD68^+$ NLCs are a source of CCL21 homeostatic chemokine. Secreted CCL21 is retained in the NLC cell membrane, thus providing a potent chemoattractant signal for CLL B cells and favoring their retention through NLC/B cell crosstalk. Inhibition of CCL21/CCR7 interaction or use of therapeutic ibrutinib alters adhesion of leukemic cells to the protective NLC cells.

Methods

Cells and tissues

CLL blood samples were obtained from untreated patients after informed consent and validation by the local research ethics committee from the Avicenne Hospital (Bobigny, France), in accordance with the Declaration of Helsinki. Paraffin-embedded lymph nodes of patients with CLL or nontumoral pathologies were obtained from the Department of Pathology at Avicenne Hospital (supplemental Table 1).

Nurselike cells culture

PBMCs isolated by density-gradient centrifugation from patients with CLL were suspended in RPMI with 10% FCS and penicillin-streptomycin to a final concentration of 10^7 cells/mL and maintained in culture at 37°C for 14 days. When indicated, after 14 days, the cocultures were incubated with 1μM of ibrutinib (Selleckchem) for 24 hours.

Immunohistochemistry

Three-micron-thick sections of paraffin-embedded lymph node tissues were deparaffinized and rehydrated using standard histological techniques. Sections were incubated with the indicated antibodies (supplemental Table 2) and revealed using the Ventana endogenous peroxidase kit (Ventana Medical Systems, Tucson, AZ) according to the manufacturer's instructions.

Immunofluorescence

Tissue sections were dewaxed by immersion in xylene and hydrated by serial immersion in ethanol and phosphate-buffered saline (PBS). Antigen retrieval was performed by heating sections for 10 minutes in 10 mM of sodium citrate buffer, pH 6.0, and blocking for 10 minutes in 2% BSA (Bovine Serum Albumine). Sections were incubated with the indicated primary and secondary antibodies for 1 hour (supplemental Table 2). Colocalization between FRC and CCL21 or $CD68^+$ cells and CCL21 was quantified after development of an image-processing algorithm in ImageJ.

mRNA and protein detection

Prime-Flow RNA assay was performed using the assay kit from Thermo Fisher Scientific (Carlsbad, CA) according to the manufacturer's instructions. Nonadherent cells were removed from the

culture after 14 days by vigorous pipetting, and the remaining adherent cells were harvested using 5 mM of EDTA/PBS. Cells were stained for the indicated surface and intracellular markers. Cellular RNA targets were detected by sequential hybridizations with target probe sets (supplemental Table 2). Further details are given in supplemental Methods.

Imaging flow cytometry

For each sample, 40 000 cells were analyzed on a three-laser ImageStreamX imaging flow cytometer (Amnis, Seattle, WA) with a 40× objective (0.75 NA) using the INSPIRE (Amnis) software. Post-acquisition data analysis was performed using IDEAS 3.0 software (Amnis).

CLL B-cell motility and retention

After 14 days, adherent NLC cells were harvested with 5 mM of EDTA/PBS and seeded overnight in Ibidi μ-slides (Ibidi, Gräfelfing, Germany). Nonadherent B cells were removed and kept at 37°C. The next day, NLCs were incubated or not with a blocking anti-CCL21 antibody (4 μg/mL, 30 minutes at 37°C) and then stained with 125 nM of calcein red orange (10 minutes at 37°C; Invitrogen). B cells were incubated or not with either blocking anti-CCR7 Abs (10 μg/mL; 30 minutes at 37°C) or blocking anti-CXCR4 and anti-CXCR5 Abs (30 μg/mL and 20 μg/mL, respectively; 1 hour at 4°C), stained with 0.5 μM of 5-chloromethylfluorescein diacetate (CMFDA, Invitrogen); (10 minutes at 37°C), and finally resuspended in the 14-day culture medium or in fresh medium. When indicated, NLC and B cells were treated with 1 μM of ibrutinib for 24 hours and B cells were resuspended in 14-day culture medium after staining. Four thousand B cells were added to their autologous NLCs and imaged. Images were acquired every 20 seconds for 20 minutes using an inverted widefield microscope (Eclipse TE2000-U; Nikon). Cellular motility parameters were then calculated using Trackmate (ImageJ).

Slides were then incubated for 4 hours at 37°C and repeatedly washed before acquiring further images.

Statistics

P values were calculated using the paired or unpaired tests (two-tailed, 95% CI) by GraphPad Prism software (GraphPad Software Inc., San Diego, CA).

Results

FRC and FDC networks are disrupted in CLL lymph nodes

Stromal cell organization in lymph node biopsies from patients with CLL was compared with biopsies from nontumoral vascular surgery. As expected, in nontumoral lymph nodes the distribution of the CCL21 chemokine positive cells corresponded to α smooth muscle actin (αSMA) positive network of FRC. Meanwhile $CXCL13^+$ cells were superimposable to the $CD21^+$ network of FDCs (Figure 1A, panels a-d). In almost every tumoral CLL lymph node, this subtissular organization was lost. Several isolated αSMA^+ cells persisted without distinguished organization as an FRC network (Figure 1A, panel f), whereas $CD21^+$ FDCs completely disappeared (Figure 1A, panel h). Consequently, $CCL21^+$ and $CXCL13^+$ cells were randomly distributed (Figure 1A, panels e,g) over a diffuse lymphoid proliferation in CLL in contrast with a strong localization in the germinal center in nontumoral samples (supplemental Figure 1A, panels a,d). Specifically, a massive infiltration of $CD20^+$ cells and a dispersed and reduced distribution of $CD3^+$ cells were detected in CLL biopsies (supplemental Figure 1A, panels e-f).

We also observed an enrichment in $CD68^+$ cells in all tumoral cases of our series compared with nontumoral biopsies (Figure 1B). An evaluation of the $CD68^+$ cells showed a significantly higher density of these cells in the tumor infiltrate compared with the nontumoral compartment (outside sinuses) for the various biopsies tested in the study ($n = 10$ of each case; $P < .005$) (Figure 1C).

Overall, our results showed that FRC network was disrupted in the lymph nodes from patients with CLL while FDC almost disappeared. Concomitantly, we observed an increase in $CD68^+$ cell population randomly distributed on the lymphoid proliferative cells.

Both FRC and $CD68^+$ cells produce CCL21 in CLL lymph nodes

In line with this relevant disorganization of lymph nodes, we addressed the identification of $CCL21^+$ cells in the tumor microenvironment and asked whether they might correspond at least partly to $CD68^+$ cells or were only representative of residual FRCs. Therefore, we compared the distribution of CCL21 expressing cells among $CD68^+$ cells and ER-TR7–labeled FRCs in lymph node sections from nontumoral and CLL samples ($n = 8$ from each one) using immunofluorescence methodologies. Confocal images confirmed the increase of $CD68^+$ cells and the loss of an organized FRC network in CLL samples as previously observed by immunohistochemistry. Merged images showed that CCL21 colocalized almost exclusively with FRC staining in control samples whereas CD68 labeling remained isolated (Figure 2A, FRC/CCL21 magenta and CD68 green, respectively, in nontumoral merge panel). Conversely, in CLL samples, CCL21 signal colocalized with both $CD68^+$ cells and FRCs (Figure 2A, CD68/CCL21 yellow and FRC/CCL21 magenta, respectively, in CLL merge panel). The colocalization was further quantified using an image processing tool. Upon image capture, a mask for each fluorescence signal was developed. A significantly increased number of CD68-specific pixels was detected in CLL samples compared with nontumoral samples, confirming the increase of $CD68^+$ cells. Conversely, some nonsignificant decreases were observed for FRC or CCL21 signals between samples (supplemental Figure 1B). Next, additional masks combining CCL21 with either FRC^+ (ER-TR7) or $CD68^+$ signals were created. White pixels matched with positivity in both channels whereas isolated $CCL21^+$ labeling remained red (Figure 2B). Indeed, white pixels were mainly observed for FRC in nontumoral tissues and were randomly distributed between FRC and $CD68^+$ cells in CLL samples. Importantly, the specificity of the staining was proved with a strong inverse exclusion for CCL21 expression between $CD68^+$ cells and FRCs (Figure 2B). A measure of the percentage of colocalization was obtained by computing the number of merged pixels. We then compared the ratios between merged CCL21/FRC and CCL21/CD68 pixels relative to the total number of $CCL21^+$ cells in nontumoral or CLL samples. The colocalization CCL21/CD68 was significantly higher in CLL samples and was concomitant with a decreased CCL21/FRC colocalization (Figure 2C, left graph) This result indicated that in CLL lymph nodes an important proportion of CCL21

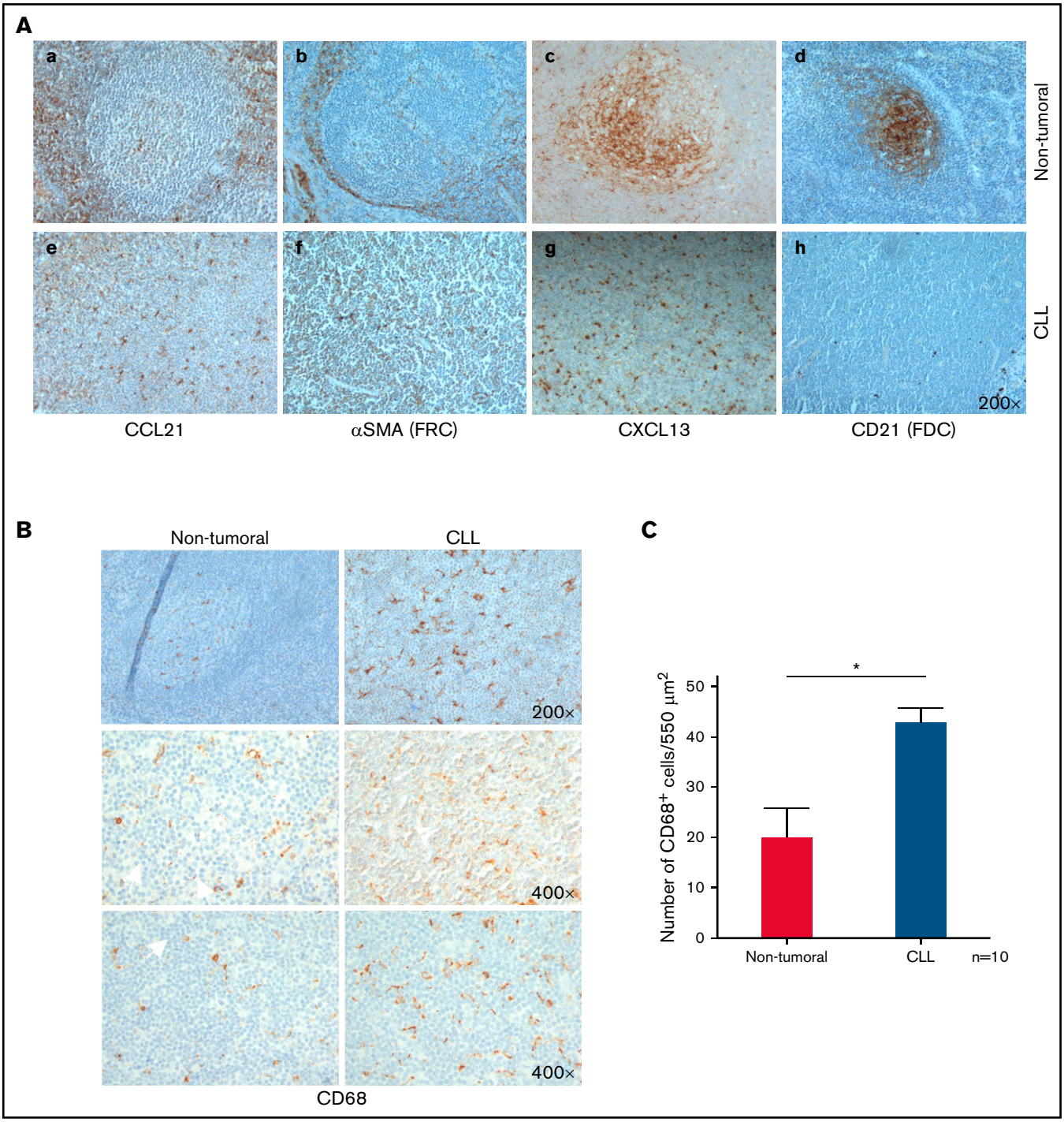

Figure 1. Disorganization of FRC/FDC networks and increase of CD68$^+$ macrophages in CLL lymph nodes. (A) Representative images from nontumoral (panels a-d) and CLL (panels e-h) lymph node tissue sections. Immunohistochemical staining was used on samples (anti-CCL21 and anti-αSMA or anti-CXCL13 and anti-CD21 antibodies), representative of FRC and FDC (original magnification ×200). (B) Representative images from nontumoral (left panels) and CLL (right panels) lymph node tissue sections stained with anti-CD68 antibody (original magnification ×200 and ×400, respectively). (C) Quantification of CD68$^+$ cells per 550 μm^2 section in nontumoral (n = 10) and CLL lymph nodes (n = 10); statistical analysis was carried out by Student *t*-test (*$P < .005$). Images were acquired using a DFC 300 FX Leica microscope with a ×10 objective.

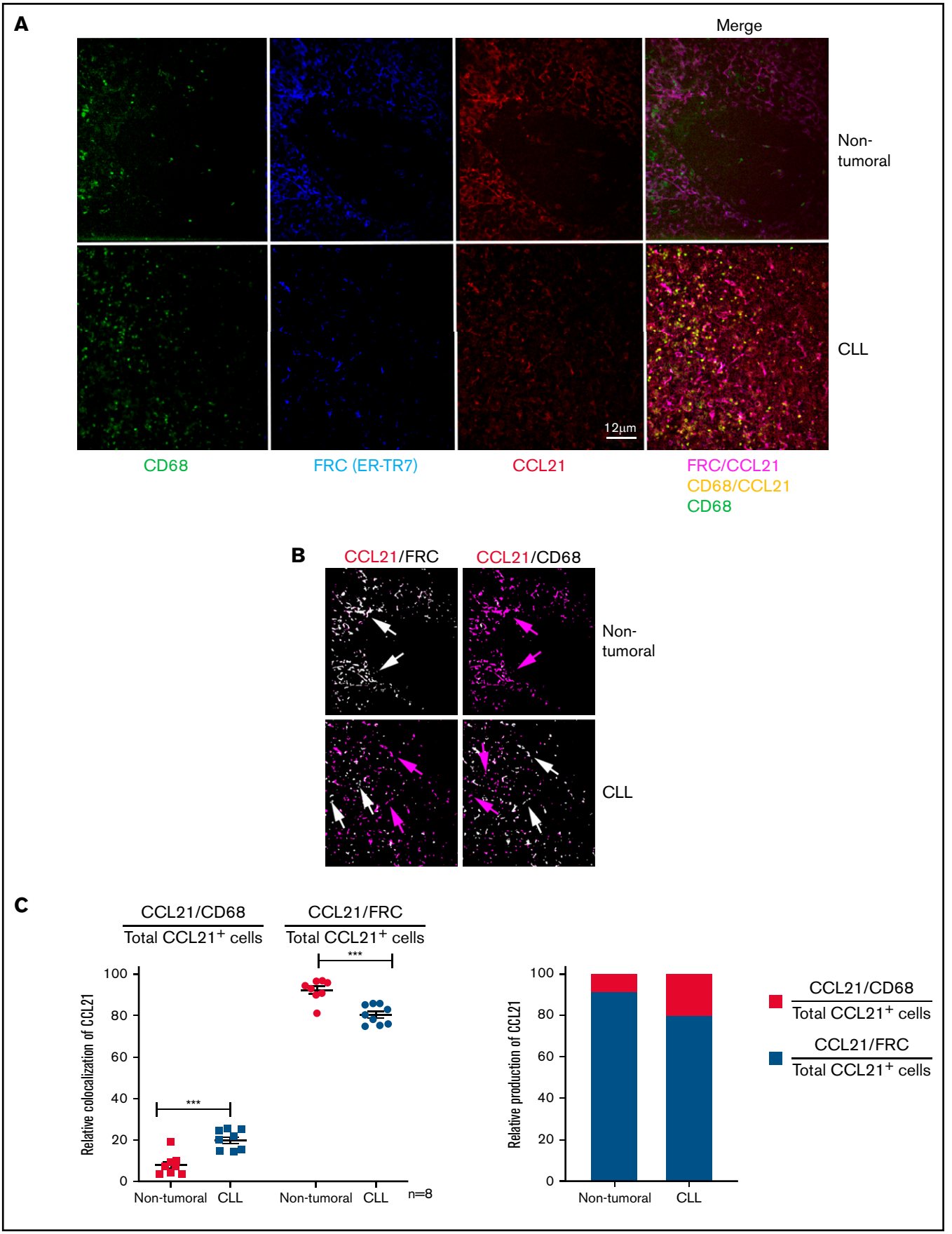

Figure 2.

was produced by CD68$^+$ cells whereas the remaining FRCs could still produce CCL21 (Figure 2C, right graph).

CD68$^+$ nurselike cells produce CCL21 that is specifically retained at the cell membrane

Previous studies indicated a prosurvival role for peripheral blood–derived CD68$^+$ macrophages in coculture with CLL B cells. These so-called NLCs mimic the protective niches observed in lymph nodes.[21] We investigated the production of CCL21 by NLCs in vitro differentiated from PBMCs of patients with CLL (supplemental Figure 2A). After removal of the nonadherent cells, the remaining cells were harvested and analyzed by imaging flow cytometry. This approach allowed not only a quantitative analysis but also a visualization of interacting cells. Interestingly, the interaction between macrophages and B cells persisted even after a detaching intensive washing, and the aggregates could be distinguished from single macrophages in "area" versus "aspect ratio" plotting (Figure 3A). All the single CD68$^+$ macrophages expressed CD206, a typical marker of TAMs (Figure 3B). Conversely, expression of another M2-TAM typical marker, CD163, revealed highly heterogeneous proportions of positive cells among different patients, suggesting variable degrees of maturation (Figure 3B; supplemental Figure 2B).

We further used the single-cell approach, referred to as the Prime Flow RNA assay, which allowed simultaneous detection of CCL21 mRNA and protein in combination with immunophenotyping for cell surface and intracellular proteins.[22] First, the specificity of the mRNA probe was confirmed using both primary FRC cells issued from nontumoral lymph nodes and the CCL21$^+$ MDA-MB231 cell line[23] (supplemental Figure 2C). In CD68$^+$CD163$^+$ macrophages from 6 different patients, both CCL21 mRNA and protein were detected in most cells. However, an mRNA$^-$/protein$^+$ subpopulation was also observed, likely reflecting cells that no longer transcribe CCL21 but still hold substantial amounts of protein due to the presence of brefeldin in the procedure (Figure 3C, upper panel; supplemental Figure 2D, upper graph). Several CD68$^+$CD163$^-$ macrophages presented with an additional subset of cells in which only CCL21 mRNA was observed (Figure 3C, lower panel; supplemental Figure 2D, lower graph), further arguing for different degrees of maturation among the subpopulation. Imaging of the aggregates composed of CD68$^+$ and B cells demonstrated the production of CCL21 mRNA and protein in macrophages exclusively (Figure 3D). Accordingly, CCL21 mRNA was not detected in B cells issued from the suspension of PBMCs in culture for 14 days (supplemental Figure 2E).

Interestingly, in these imaging experiments, CCL21 protein was also stained at the membrane of nonpermeabilized cells and in absence of brefeldin treatment (Figure 4A). We confirmed the presence of CCL21 protein at the cell surface of adherent cells after 2 weeks of culture in both permeabilized and nonpermeabilized conditions by immunofluorescence and confocal microscopy (Figure 4B). This observation suggested that the chemokine could be captured on the cell surface upon secretion, as described for unpermeabilized lymphatic endothelium. Indeed, CCL21 appeared to be randomly distributed on CD68$^+$ cell membrane, as observed in endothelial cells.[24] Accordingly, when we analyzed chemokine secretion by the adherent NLCs after 14 days of culture, CCL21 was barely present above the detection limit whereas both CXCL13 (112.2 $\pm$ 150 pg/mL, mean $\pm$ SD; n = 14) and CXCL12 (54.2 $\pm$ 33 pg/mL, mean $\pm$ SD; n = 14) chemokines were present at various extents (Figure 4C), as previously described.[15] Correspondingly, CXCL13 mRNA was detected in adherent CD68$^+$ cells (Figure 4D).

Interestingly, gating of the aggregates showed that CD19$^+$ B cells surrounding CD68$^+$ macrophages expressed CCR7, the CCL21 receptor (Figure 4E). Furthermore, CCR7 expression levels were significantly higher in CD19$^+$ cells still present in the adherent fraction compared with those in suspension (Figure 4F). Also, we observed that CD19$^+$CD5$^+$ cells interacting with CD68$^+$ cells showed a significantly increased level of activated pY759 PCLγ2 compared with CD19$^+$CD5$^+$ cells still present in the adherent fraction but separated from NLCs or CD19$^+$CD5$^+$ cells in suspension (supplemental Figure 2F).

Altogether, these results indicated that CD68$^+$ adherent cells, upon differentiation from CLL PBMCs, produce the CCL21 chemokine that is captured on cell membrane. Furthermore, they argue for CD68$^+$ cells retaining CCR7$^+$ B cells, which would explain the strong interaction observed between macrophages and B cells.

CLL B-cell trafficking depends on secreted chemokines

To investigate the impact of CD68$^+$ NLCs in CLL B cell trafficking, we analyzed the mobility of B cells cocultured with NLCs. After 14 days of PBMC differentiation, B cells in suspension were recovered, fluorescently stained, and plated onto their autologous NLC monolayer. We first recorded their motility using time-lapse microscopy for 20 minutes. B cells that were resuspended in the 14-day culture medium (conditioned medium) showed sustained motility and random displacements near the adherent cells (supplemental Video 1; Figure 5A, gray area). Conversely, a reduction of the mean speed was observed when B cells were resuspended in fresh medium, namely deprived of any factor produced during the 14 days of culture (supplemental Video 2; Figure 5A, yellow area). Indeed, analysis of the supernatants by Luminex showed heterogenous levels of CXCL13 in all samples whereas CXCL12 was detected only in several samples. As previously observed, CCL21 was not detected above threshold (supplemental Figure 3A). The presence of CXCR4, CXCR5, and CCR7 on B cells was also measured, showing heterogenous expression levels (supplemental Figure 3B).

Figure 2 (continued) CCL21 is produced by FRCs and CD68$^+$ cells. (A) Representative images from nontumoral (upper panels) and CLL (lower panels) lymph node sections stained with anti-CD68 (green), anti-ER-TR7 (blue), or anti-CCL21 (red) antibodies (objective $\times$63; scale bar represents 12 μm) and merged images in pink (FRC/CCL21) or yellow (CD68/CCL21). Images were acquired using a DMI6000 Leica Spinning Disk microscope with a $\times$40 1.25NA objective (Leica Microsystems, Wetzlar, Germany) and a Photometrics Coolsnap HQ CCD, driven by Metamorph software (Molecular Devices, Sunnyvale, CA) at the Imaging Facility of Cochin Institute, Paris, France. (B) Masks created from the images in panel A by combining FRC and CCL21 signals or CD68 and CCL21 signals. Pixels are white when both channels are positive and pink when CCL21 is alone. (C) Graph comparing the ratios between colocalized CCL21/CD68 or CCL21/FRC pixels and the total number of CCL21$^+$ cells in nontumoral and CLL samples. Measure of the colocalization was obtained by computing the total number of positive pixels. Means were compared in a Student *t*-test (**P = .0026; n = 8).

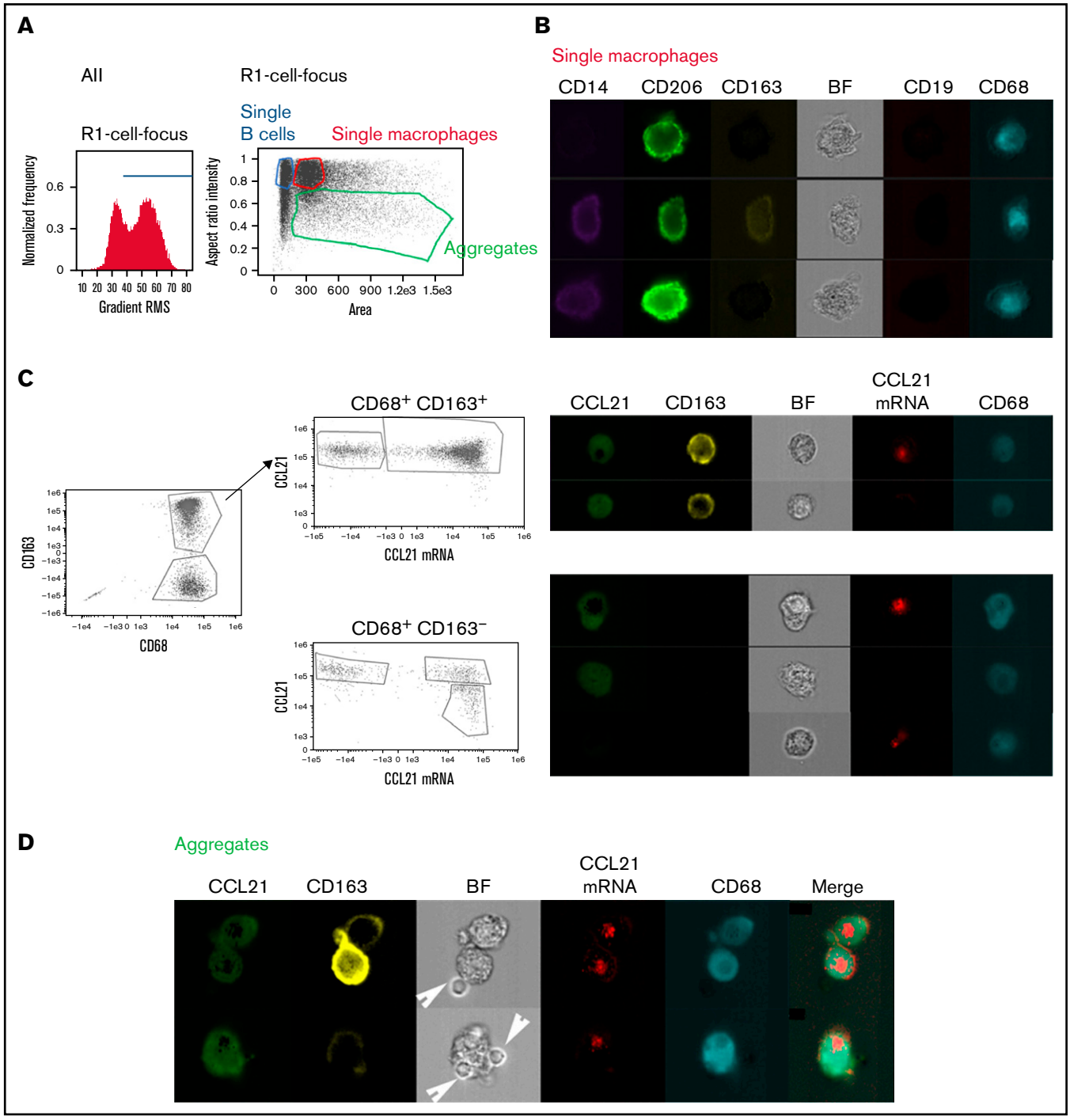

Figure 3. CD68$^+$ NLCs produce CCL21. (A) Assay outline and gating strategy applied to identify single cells and aggregates. Cells in camera focus were selected from all events on the basis of gradient RMS of the bright field image. Single B cells, macrophages, and cellular aggregates were identified by plotting "area" vs "aspect ratio" in which events with higher aspect ratio are assigned to single cells while those with lower aspect ratio are aggregates. (B) Image gallery of single macrophages showing different subpopulations based on CD14 (purple), CD206 (green), CD163 (yellow), CD19 (red), and CD68 (cyan) fluorescent signals as well as Brightfield (BF). (C) Detection of CCL21 mRNA and protein in CD68$^+$ CD163$^+$ or CD68$^+$ CD163$^-$ subpopulations. Galleries show CCL21 protein (green), CD163 (yellow), CCL21 mRNA (red), and CD68 (cyan) fluorescent signals as well as Brightfield (BF). (D) Image gallery of aggregates of macrophages and B cells showing CCL21 (green), CD163 (yellow), CCL21 mRNA (red), and CD68 (cyan) fluorescent signals as well as Brightfield (BF). Arrows show B cells present in the aggregates. Merged images show that B cells are negative for CCL21 and CCL21 mRNA signals. All the experiments were performed in permeabilized cells after brefeldin (BFA) treatment.

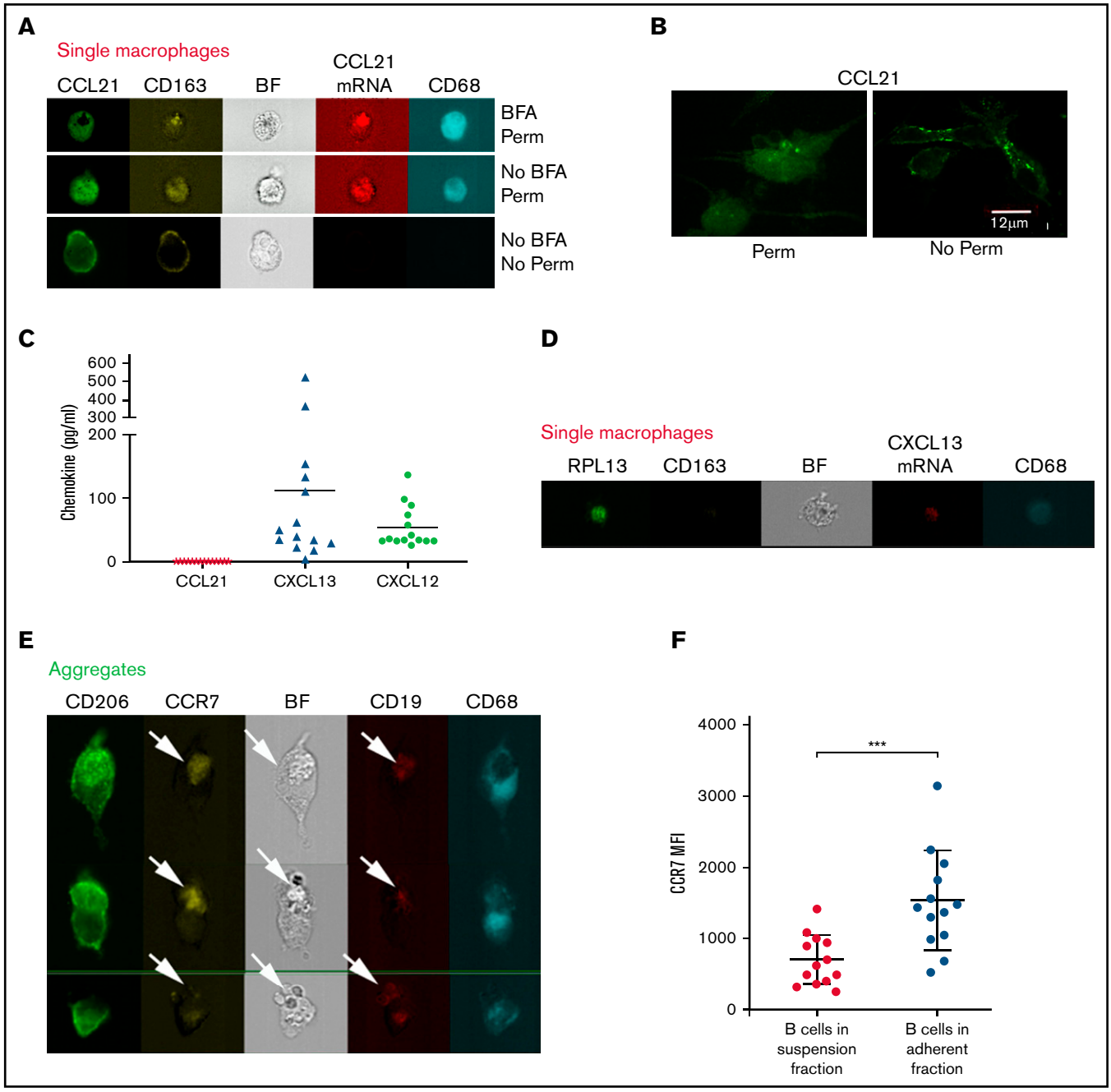

Figure 4. CCL21 is retained on cell membrane and not detected in the supernatant. (A) Image galleries of single macrophages (as defined in panel 3A) showing CCL21 (green), CD163 (yellow), CCL21 mRNA (red), and CD68 (cyan) fluorescent signals and Brightfield (BF) in permeabilized (upper and middle) and nonpermeabilized (lower) conditions in presence (upper) or absence (middle and lower) of BFA treatment. (B) Confocal images of adherent $CD68^+$ cells stained with anti-CCL21 Ab in permeabilized (left) or nonpermeabilized (right) conditions (objective ×63; scale bar represents 12 µm). (C) CCL21, CXCL13, and CXCL12 protein levels secreted by adherent NLCs after 14 days of culture detected by Luminex technology. Dots represent individual protein levels from 14 patients with CLL. (D) Detection of CXCL13 mRNA in single macrophages. Image galleries of single macrophages showing RPL13 mRNA (green), CD163 (yellow), CXCL13 mRNA (red), and CD68 (cyan) fluorescent signals and Brightfield (BF). RPL13 mRNA of ribosomal protein L13A was used as housekeeping control. (E) Image gallery of aggregates showing macrophages and B cells based on CD206 (green) and CD68 (cyan) or CCR7 (yellow) and CD19 (red) fluorescent signals, respectively, as well as Brightfield (BF) in permeabilized conditions. Arrows show B cells present in the aggregates. (F) Graph shows the CCR7 MFI (Mean Fluorescence Intensity) values detected on B cells in suspension or remaining in the adherent fraction after 14 days of culture.

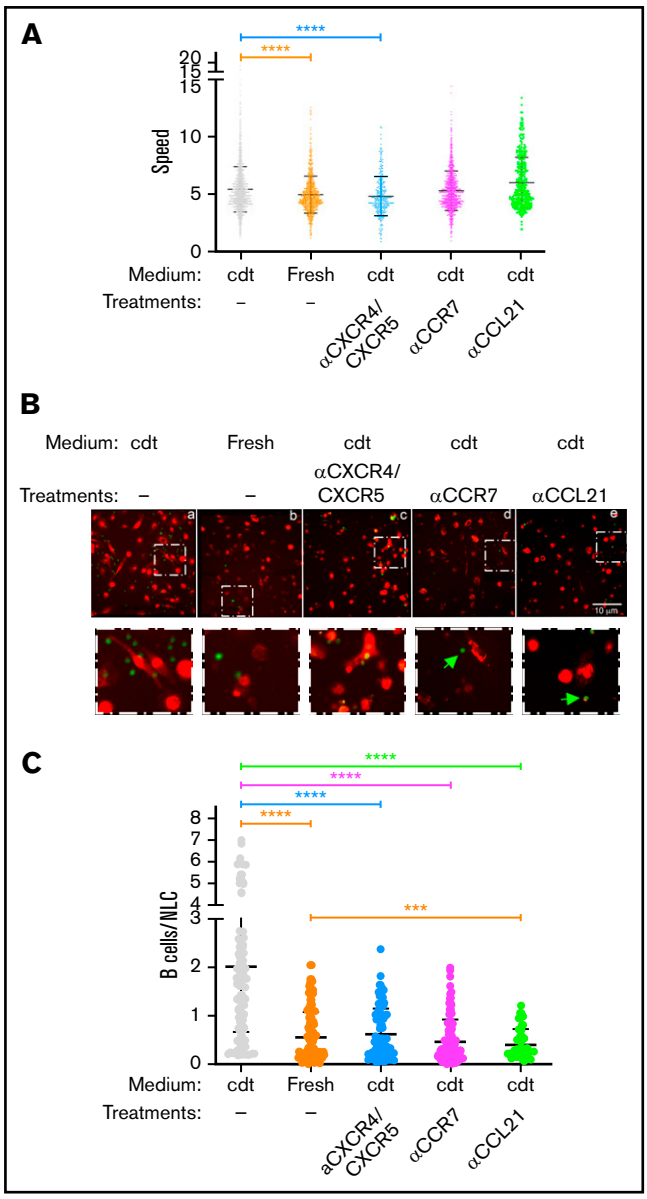

Figure 5. Chemokines produced by NLCs impact B cell motility. (A) Graph comparing the mean speed of B cells loaded on NLC monolayers in 14-day culture-conditioned medium (cdt) or fresh medium. B cells were left untreated or incubated with anti-CCR7 (10 μg/mL), anti-CXCR4 (30 μg/mL), and anti-CXCR5 antibodies (20 μg/mL) before loading. CD68$^+$ NLCs were incubated or not with anti-CCL21 antibody (4 μg/mL) before addition of untreated B cells. Motility was analyzed using Trackmate in ImageJ software. Only displacement lengths >10 μm were included in the analysis (n = 12). (B) Representative images of interactions between CLL B cells (green) and CD68$^+$ NLCs (red) after 4 hours of coculture in conditions identical to panel A and vigorous washing (objective ×20; scale bar represents 10 μm). The areas in the white dotted boxes in the upper panel are ×3.5 zoomed in the lower panels to show B/NLC interactions. Green arrows show noninteracting B cells. (C) Graph comparing the ratios of colocalized B cells/NLCs detected in the different conditions. Postacquisition data analysis of images in panel B was performed using ImageJ software. To quantify B cells in contact with NLCs, a threshold was applied to obtain a mask of NLCs, and the number of B cells present in this mask was evaluated using the "analyze particles" tool and represented in the graph as number of B cells per NLC. Statistical analysis was carried out by Student *t*-test (***$P < .001$; ****$P < .0001$; n = 12).

The impact of their specific blocking by inhibitory antibodies was then analyzed. Prevention of MAPK/ERK activation upon binding of the respective chemokines attested to inhibition in the presence of the antibodies (supplemental Figure 3C). We then simultaneously blocked CXCR4 and CXCR5 receptors on B cells before loading them in conditioned medium, and a substantial reduction of their velocity was observed comparable to loading in fresh medium (supplemental Video 3; Figure 5A, blue area). On the contrary, mean speed did not significantly decrease after blocking of CCR7 receptor on B cells and increased after blocking of CCL21 on NLC cells (supplemental Videos 4 and 5; Figure 5A, pink and green areas, respectively).

Because the therapeutic BTK inhibitor ibrutinib has been involved in both direct targeting of the tumor cells and tumor–microenvironment interactions critical for CLL progression,[25,26] its impact on B cell mobility was investigated. As previously described,[26,27] we first confirmed that PBMCs from patients treated with ibrutinib could generate differentiated NLCs in vitro (supplemental Figure 4A). Furthermore, NLCs maintained their capacity to preserve CLL cells from ex vivo spontaneous apoptosis. CLL cells cultured alone were sensitive to ibrutinib treatment whereas culture with NLCs protected the tumor cells from ibrutinib-induced apoptosis (supplemental Figure 4B). We further verified that exposure of NLCs to ibrutinib for 24 hours interfered with BTK activation, as determined by decreased phosphorylation levels at both Tyr223 and Tyr551 sites (supplemental Figure 4C). Mobility of the cocultures exposed for 24 hours to ibrutinib prior to time lapse evaluation did not show significant changes in Bcell mean speed. Similarly, B cells from patients treated with ibrutinib showed comparable speed in these experimental settings (supplemental Figure 4D). Indeed, analysis of the culture supernatants by Luminex confirmed the heterogeneity of CXCL13 and CXCL12 expression between samples that was not affected by ibrutinib treatment. Similarly, CXCR5 and CXCR4 expression levels were not impacted (supplemental Figure 4E-F).

These results showed that CD68$^+$ NLCs impact B cell motility. Specifically, CXCL12 and CXCL13 secreted by NLC cells contribute to moving of B cells among the surrounding NLCs. This chemokine-dependent motility was not affected by ibrutinib treatment.

CCL21 chemokines retained at the NLC membrane impact formation of contacts with B cells

We then analyzed B cell interaction with NLC cells. After image recording, cocultures in the various experimental settings were incubated for 4 hours and the presence of remaining B cells was evaluated after vigorous washing. In untreated conditions, the presence of B cells interacting with NLCs was detected (Figure 5B, panel a). In contrast, a substantial reduction of B cells, still interacting with NLCs, was observed when cells were resuspended in fresh media as well as upon CXCR4/CXCR5 before blocking (Figure 5B, panels b-c). More importantly, few B cells could be detected upon CCR7 blocking on B cells or CCL21 blocking on NLCs. Interestingly, in the latest conditions, the residual B cells present did not directly interact with NLCs (Figure 5B, panels d-e). These interactions were quantified by creating masks to detect B- and NLC cell signals and combine them when overlapping. The B cell/NLC ratio represented colocalization of B cells with adherent NLCs. The quantification of 12 samples confirmed the significative differences

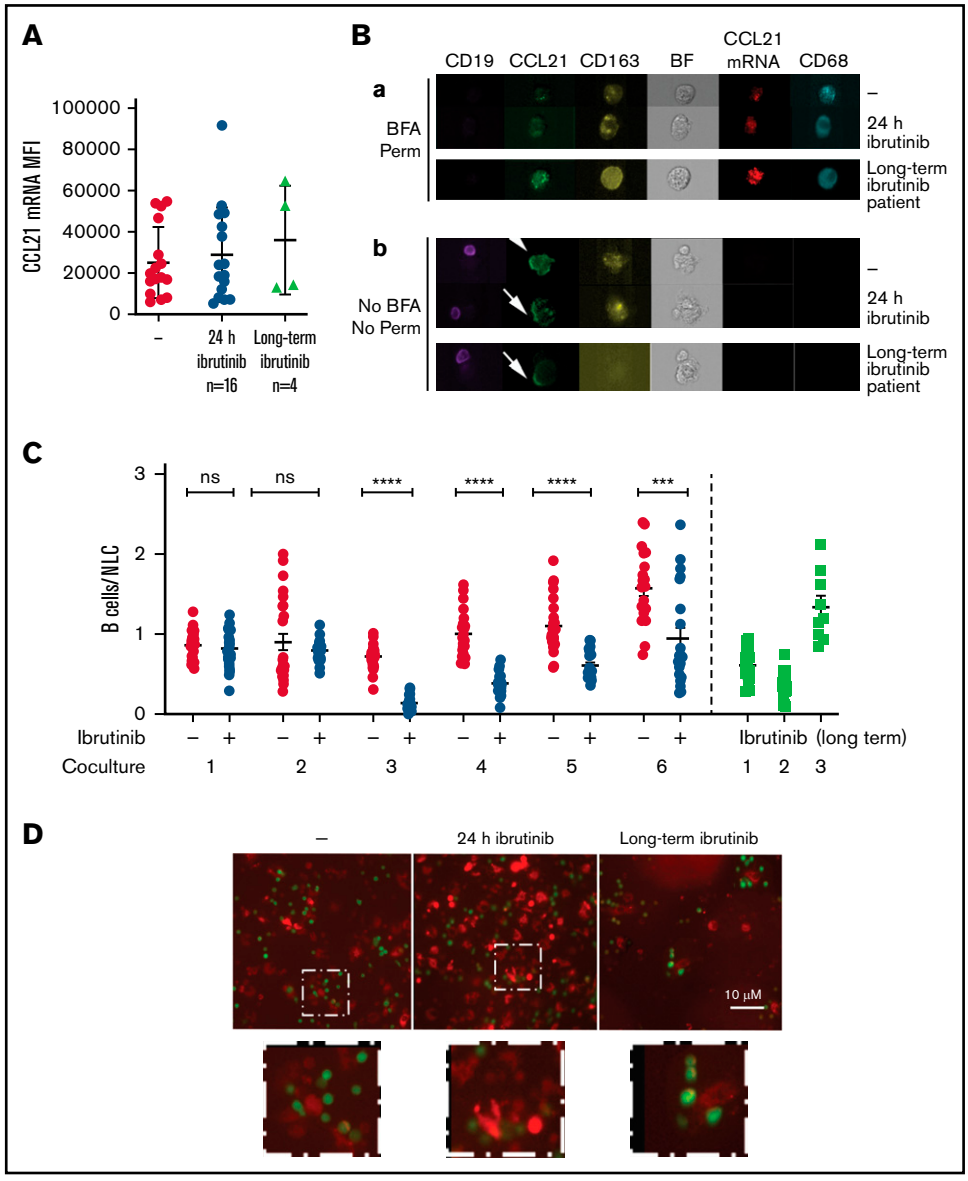

Figure 6. Ibrutinib impacts B cells/NLC interaction. (A) Graph shows the CCL21mRNA MFI values detected in NLC cells exposed or not to ibrutinib 24 hours before analysis (P = ns; n = 16) or in NLCs derived from patients treated with ibrutinib (n = 4). (B) Image galleries of single macrophages or aggregates (as defined in Figure 3A) exposed or not to ibrutinib for 24 hours (upper panels) or derived from patients treated with ibrutinib (lower panels) showing CD19 (purple), CCL21 (green), CD163 (yellow), CCL21 mRNA (red), and CD68 (cyan) fluorescent signals and Brightfield (BF) in permeabilized conditions and in presence of BFA (a) or nonpermeabilized conditions and no BFA treatment (b). (C) Graph comparing the ratios of colocalized B cells/NLCs after 4 hours of coculture exposed (+) or not (−) to ibrutinib for 24 hours (n = 6) or in cocultures derived from patients treated long-term with ibrutinib (n = 3). Statistical analysis was carried out by Student t-test (***$P < .001$; ****$P < .0001$) comparing untreated and treated samples. (D) Representative images of interactions between CLL B cells (green) and CD68$^+$ NLCs (red) after 4 hours of coculture priorly treated or not with ibrutinib (24 hours) or in cocultures derived from patients treated with ibrutinib (objective ×10; scale bar represents 10 µm). The areas in the white dotted boxes in the upper panel are ×2.5 zoomed in the lower panels to show B cell/NLC interactions.

observed, particularly confirming the loss of interaction after CCL21 inhibition (Figure 5C).

We finally investigated the impact of ibrutinib on CD68$^+$ NLC/CLL B cell direct interaction by exposing the coculture to ibrutinib for 24 hours before analysis or using a coculture with NLC/B cells derived from patients treated with ibrutinib. In these experiments, ibrutinib in vitro exposure did not alter CCL21 mRNA expression in NLC cells, as shown by similar CCL21 mRNA MFI (Mean Fluorescence Intensity) in untreated and treated samples, nor did it alter samples from long-term treated patients (Figure 6A-B, upper panel a). Also, CCL21 proteins were detected on the membrane of nonpermeabilized cells in both untreated and ibrutinib-treated samples as well as on cells from long-term treated patients (Figure 6B, lower panel b). These results suggest that Ibrutinib does not directly target CCL21 production by NLCs. The quantification of B/NLC interactions after 4-hour incubation of the different cocultures showed that 4 out of 6 ibrutinib-treated samples and 2 out of 3 long-term treated patient

samples displayed a significant reduction of colocalization (Figure 6C-D). On the other hand, B cells still able to interact with NLCs were observed in the various experimental settings (Figure 6D), and CCR7 expression levels at their surface were not affected by ibrutinib treatment (supplemental Figure 4F).

These results shed light on the role of CCL21, retained at NLC membrane, playing a role in the interaction with CCR7-expressing B cells, likely favoring their capture by NLCs. Overall, these observations suggest a cooperative impact of soluble and membrane chemokines produced by NLCs in B cell trafficking and retention in lymphoid organ niches.

Discussion

Malignant progression of CLL cells regarding cell survival and proliferation, migration, or retention as well as resistance to therapeutic treatment is impacted by signals emanating from the surrounding cells in protective niches such as lymphoid organs. Understanding the complex interplay between CLL and neighboring cells is still sparse while the important alterations of lymph node architecture must be taken into account. Here, we performed an analysis of the cellular organization in CLL lymph nodes. We described fully disorganized substructures, with disruption of the FRC network leaving only residual stretches, loss of FDCs, absence of the B cell follicles, and T-cell–zone and large infiltration of the leukemic cells in every compartment. Meanwhile, we observed a significantly increased presence of $CD68^+$ cells with the characteristics of NLCs. NLCs induce chemotaxis and promote survival of CLL cells, notably through the secretion of distinct chemokines and prosurvival factors. We showed here, for the first time, that $CD68^+$ NLCs produce the homeostatic chemokine CCL21 as well as CXCL12 and CXCL13, two chemokines already described for their role in B cell homing and differentiation in the BM. In lymph nodes, these chemokines also play a critical role in affinity maturation and formation of germinal center.[15,28] CCL21 and its cognate receptor CCR7 are important players in CLL transmigration across HEVs into the lymph nodes. Indeed, CCL21 is a potent B cell chemoattractant,[17] and knockout mice for CCR7 display defective B cell entry into lymphoid secondary organs.[18] Furthermore, the levels of CCR7 on B cells were significantly higher in patients presenting with lymphadenopathy, thus associating this interacting capacity with the proliferative niches in CLL.[20,29,30] Our results shed light on the CCL21/CCR7 axis as being involved not only in the entry but also in the retention and the accumulation of malignant B cells in pathological lymph nodes. CCL21 is produced by lymphatic endothelial cells in peripheral tissues,[24,31] by HEV,[20,32] and by FRCs in the T cell zone of lymph nodes.[33] Our immunofluorescence analyses showed $CD68^+$ cells able to express CCL21 in lymph node sections. The significant increase of $CD68^+$ cells in lymph nodes from patients with CLL paralleled the loss of FRC network organization, which creates the assumption that $CD68^+$ cells represent an additional and alternative source of CCL21 supplanting the role attributed to FRCs. A similar role for $CD68^+$ cells substituting FDC production of CXCL13 has been described in lymphocytic lymphoma.[15]

We demonstrated specific CCL21 production by detecting both CCL21 mRNA and protein in single $CD68^+$ cells obtained after in vitro differentiation of PBMC-derived monocytes from patients with CLL.[5] This in vitro model was used to circumvent our lack of accessibility to fresh tumor tissues, allowing sorting of $CD68^+$ cells. We used an imaging flow cytometry approach, which allows not only quantitative analysis but also simultaneous visualization of mRNA and protein expression within a single cell and cell–cell interactions. Indeed, in coculture experiments and despite intensive washes, we obtained persistent aggregates composed of $CD68^+$ cells interacting with B cells. Interestingly, B cells retained on NLC cells showed a higher activation according to higher phospho-PLCγ2 expression, in comparison with noninteracting B cells. This observation argues for the protective role of NLCs in niching zones. The imaging approach let us distinguish single macrophages, isolated B cells, or aggregates, and CCL21 production was exclusively attributed to $CD68^+$ cells in those circumstances. Interestingly, immunofluorescence analysis on lymph node sections showed that CCL21 staining was spread all along the cellular membrane. This pattern was comparable to the intracellular depots of the chemokine within lymphatic endothelium described by Weber et al.[24] Indeed, CCL21 has a highly charged C-terminal extension that binds glycosaminoglycans, and it is presumed responsible for immobilizing the chemokine to extracellular matrix or cell surface.[34,35] Using imaging cytometry and confocal microscopy, we also detected CCL21 protein in unpermeabilized in vitro differentiated NLCs and observed it on their cell membrane. Accordingly, CCL21 proteins in the culture supernatants were under the detection threshold whereas CXCL13 and CXCL12 were present at heterogenous levels. This result suggested that CCL21, once secreted by $CD68^+$ cells, might be kept on their cell surface and subsequently may retain $CCR7^+$ B cells. For this, we analyzed the mobility behavior of B cells loaded on a monolayer of adherent $CD68^+$ cells. We observed that the motility of B cells in the vicinity of adherent $CD68^+$ cells was deeply affected when a fresh medium was used. This medium was particularly deprived of factors such as CXCL13 and CXCL12. A similar effect was observed after blocking their cognate receptors, CXCR5 and CXCR4, on B cells. Although the contribution of other soluble factors and the chemokine gradients present in lymphoid tissues must be taken into account, these observations suggest that soluble chemokines released from NLCs impact B-cell motility. On the other hand, blocking of CCR7 on B cells or CCL21 on $CD68^+$ cells caused a complete loss of B cells/$CD68^+$ cell interactions. Indeed, CLL B cells express more CCR7 than normal B cells. These findings give credit to our model in which CCL21 retained at the membrane plays a major role in capturing CCR7-expressing B cells and favoring their survival and activation. Indeed, we observed that B cells interacting with NLCs exhibited a higher level of activation as evaluated by PLCγ2 phosphorylation. However, this does not rule out the possible contribution of integrins to strengthen theses interactions. Notably, LFA-3 overexpression by CLL cells promotes their prosurvival interactions with CD2-expressing NLCs.[36]

Ibrutinib, a therapeutic BTK inhibitor, has been described as disrupting tumor–microenvironment interactions that are critical for CLL progression in addition to directly targeting tumor cells.[25-27] In our systems, we observed that 24-hour or long-term exposition to ibrutinib did not affect mobility of B cells. Indeed, BTK inhibition did not affect recycling and expression of chemokine receptors, especially of CCR7, on B cells nor the production of chemokines by NLCs. Specifically, expression and localization of CCL21 on NLC membranes were not altered. While reduced B cell/NLC interactions were detected, the remaining B cells still maintained the ability to adhere to NLCs. Moreover, Niemann et al suggested that ibrutinib may interfere with the extent of CLL/NLCs contact in BM on the

basis of a significant decrease in CD68$^+$ cellular extension.[25] The exact mechanism by which ibrutinib affects CCL21-mediated adhesion remains to be determined, and the contribution of other factors sensitive to ibrutinib treatment cannot be ruled out. Nevertheless, our findings agree with ibrutinib leaving fully differentiated NLCs still able to sustain CLL cells during patient therapy.[27] Accordingly, with previous reports we observed that NLCs maintained their ability to preserve CLL cells from ibrutinib-induced apoptosis, suggesting that ibrutinib treatment cannot totally counteract the indirect prosurvival effects of soluble factors such as interleukin-10.[26] Indeed, in our system, exposition to ibrutinib did not impact the secretion of prosurvival CXCL12 by NLCs nor the expression of CXCR4 on CLL B cells, thereby maintaining a protective milieu.

To counteract the chemoprotective effect induced by NLC in patients treated with ibrutinib, cotreatments with other antileukemic agents such as bendamustin or venetoclax, a Bcl-2 antagonist, showed promising results.[27] More recently, increased secretion of interleukin-10 upon ibrutinib treatment has been shown to enforce M2 phenotype of NLCs exacerbating their immunosuppressive profile. Anti–interleukin-10 in combination with classic targeting of CLL cells could be beneficial, as shown in other diseases.[37] Several other drugs inducing depolarization of M2-protective in M1-nonprotective NLCs could also pave the way for new combinatory therapies.

The analysis of CD68$^+$ NLCs differentiated from various patients showed heterogeneous proportions of CD163$^+$ cells. Interestingly, when we analyzed the presence of CCL21 mRNA and protein, we reproducibly observed a subset of CD163$^-$ cells expressing only CCL21 mRNA, which suggests different degrees of differentiation for these cells. CD163 has been proposed as a bona fide marker of M2-NLCs. Specifically, the presence of CD163$^+$ NLCs was correlated with CLL proliferative niches in lymph nodes, and high levels of soluble CD163 were linked to worse prognosis of the disease.[38] Moreover, ibrutinib treatment exacerbated the expression of M2 polarization, particularly of CD163 and CD206 markers.[26] Recently, in Richter syndrome, a transformation of CLL into an aggressive lymphoma, a higher infiltration of CD163$^+$ macrophages was observed in nodal tissue as compared with CLL.[39] Thus, our results support the relevance of CD163 expression as a final NLC differentiation marker and, likely, fully activated cells.

Overall, our study provides a description of the major changes to lymph node architecture upon massive tumor B cell infiltration, particularly with a loss of FRC network organization. In this context, we demonstrated that CD68$^+$ NLCs produce CCL21, showing that these cells are an alternative source of the chemokine, taking over the regular role of FRCs, in destructured CLL lymph nodes. In turn, CCL21 plays a critical role in capturing malignant B cells, thus favoring their niching, survival, and resistance to treatments. This evidence underlines how leukemic cells manipulate and reprogram the tumor microenvironment to create an immunosuppressive milieu that allows immune survey evasion. Moreover, these results argue for new possible combination immunotherapeutic strategies to specifically target or reprogram both CLL cells and the tumor microenvironment to effectively disrupt the protective milieu.

Acknowledgments

The authors would like to acknowledge Béatrice Durel, Pierre Bourdoncle, and Thomas Guilbert at the Platform IMAG'IC, Institut Cochin, Paris; Karine Bailly at the Plateforme "Cytométrie et Immuno-Biologie" (CYBIO), Institut Cochin, Paris, the ImagoSeine facility, member of the France BioImaging Infrastructure supported by the French National Research Agency (ANR-10-INSB-04, Investments for the future); Camille Faure (INSERM, U1016, Institut Cochin, Paris) for providing the A-MB231 cell line; Gregory Lazarian (Service d'Hématologie Biologique, Hôpital Avicenne, Bobigny) for providing patient parameters; and Luca Simula (INSERM, U1016, Institut Cochin) for help in imaging cell motility.

This work was supported by the Labex INFLAMEX, contract ANR11 IDEX00502, and by the TRANSCAN H2020 Fire CLL. R.Z. received MERT (Ministère de l'Éducation, de la Recherche et de la Technologie) and SFH (Société Française d'Hématologie) fellowships.

Authorship

Contribution: R.Z. and L.V. performed experiments; V.C. and L.V. designed and developed the quantitative method to analyze colocalization; F.C., V.L., and A.M. provided tissue and blood samples; N.V.-B., E.Donnadieu, and A.M. supervised the research and cowrote the manuscript; and E.Dondi designed and supervised the research, performed experiments, and cowrote the manuscript.

Conflict-of-interest disclosure: The authors declare no competing financial interests.

ORCID profiles: L.V., 0000-0001-7097-7851; V.C., 0000-0001-6257-1536; E.Donnadieu, 0000-0002-4985-7254; N.V.-B., 0000-0003-2769-018X; E.Dondi, 0000-0003-0975-459X.

Correspondence: Elisabetta Dondi, UMR U978, Unité Formation et Recherche Santé Médicine et Biologie Humaine (UFR SMBH), 74 rue Marcel Cachin, 93017 Bobigny cedex, France; e-mail: elisabetta.dondi@inserm.fr; and Nadine Varin-Blank, UMR U978, UFR SMBH, 74 rue Marcel Cachin, 93017 Bobigny cedex, France; e-mail: nadine.varin@inserm.fr.

References

1. Fabbri G, Dalla-Favera R. The molecular pathogenesis of chronic lymphocytic leukaemia. *Nat Rev Cancer.* 2016;16(3):145-162.
2. van Attekum MH, Eldering E, Kater AP. Chronic lymphocytic leukemia cells are active participants in microenvironmental cross-talk. *Haematologica.* 2017;102(9):1469-1476.
3. Svanberg R, Janum S, Patten PEM, Ramsay AG, Niemann CU. Targeting the tumor microenvironment in chronic lymphocytic leukemia. *Haematologica.* 2021;106(9):2312-2324.
4. Chen YCE, Mapp S, Blumenthal A, et al. The duality of macrophage function in chronic lymphocytic leukaemia. *Biochim Biophys Acta Rev Cancer.* 2017;1868(1):176-182.

5. Tsukada N, Burger JA, Zvaifler NJ, Kipps TJ. Distinctive features of "nurselike" cells that differentiate in the context of chronic lymphocytic leukemia. *Blood.* 2002;99(3):1030-1037.

6. Nishio M, Endo T, Tsukada N, et al. Nurselike cells express BAFF and APRIL, which can promote survival of chronic lymphocytic leukemia cells via a paracrine pathway distinct from that of SDF-1alpha. *Blood.* 2005;106(3):1012-1020.

7. Deaglio S, Vaisitti T, Bergui L, et al. CD38 and CD100 lead a network of surface receptors relaying positive signals for B-CLL growth and survival. *Blood.* 2005;105(8):3042-3050.

8. Talbot H, Saada S, Barthout E, et al. BDNF belongs to the nurse-like cell secretome and supports survival of B chronic lymphocytic leukemia cells. *Sci Rep.* 2020;10(1):12572.

9. Burger M, Hartmann T, Krome M, et al. Small peptide inhibitors of the CXCR4 chemokine receptor (CD184) antagonize the activation, migration, and antiapoptotic responses of CXCL12 in chronic lymphocytic leukemia B cells. *Blood.* 2005;106(5):1824-1830.

10. Nagasawa T, Hirota S, Tachibana K, et al. Defects of B-cell lymphopoiesis and bone-marrow myelopoiesis in mice lacking the CXC chemokine PBSF/SDF-1. *Nature.* 1996;382(6592):635-638.

11. Allen CD, Ansel KM, Low C, et al. Germinal center dark and light zone organization is mediated by CXCR4 and CXCR5. *Nat Immunol.* 2004;5(9):943-952.

12. Cui XY, Tjønnfjord GE, Kanse SM, et al. Tissue factor pathway inhibitor upregulates CXCR7 expression and enhances CXCL12-mediated migration in chronic lymphocytic leukemia. *Sci Rep.* 2021;11(1):5127.

13. Möhle R, Failenschmid C, Bautz F, Kanz L. Overexpression of the chemokine receptor CXCR4 in B cell chronic lymphocytic leukemia is associated with increased functional response to stromal cell-derived factor-1 (SDF-1). *Leukemia.* 1999;13(12):1954-1959.

14. Gunn MD, Kyuwa S, Tam C, et al. Mice lacking expression of secondary lymphoid organ chemokine have defects in lymphocyte homing and dendritic cell localization. *J Exp Med.* 1999;189(3):451-460.

15. Bürkle A, Niedermeier M, Schmitt-Gräff A, Wierda WG, Keating MJ, Burger JA. Overexpression of the CXCR5 chemokine receptor, and its ligand, CXCL13 in B-cell chronic lymphocytic leukemia. *Blood.* 2007;110(9):3316-3325.

16. Saint-Georges S, Quettier M, Bouyaba M, et al. Protein kinase D-dependent CXCR4 down-regulation upon BCR triggering is linked to lymphadenopathy in chronic lymphocytic leukaemia. *Oncotarget.* 2016;7(27):41031-41046.

17. Nagira M, Imai T, Yoshida R, et al. A lymphocyte-specific CC chemokine, secondary lymphoid tissue chemokine (SLC), is a highly efficient chemoattractant for B cells and activated T cells. *Eur J Immunol.* 1998;28(5):1516-1523.

18. Förster R, Schubel A, Breitfeld D, et al. CCR7 coordinates the primary immune response by establishing functional microenvironments in secondary lymphoid organs. *Cell.* 1999;99(1):23-33.

19. Rehm A, Mensen A, Schradi K, et al. Cooperative function of CCR7 and lymphotoxin in the formation of a lymphoma-permissive niche within murine secondary lymphoid organs. *Blood.* 2011;118(4):1020-1033.

20. Till KJ, Lin K, Zuzel M, Cawley JC. The chemokine receptor CCR7 and alpha4 integrin are important for migration of chronic lymphocytic leukemia cells into lymph nodes. *Blood.* 2002;99(8):2977-2984.

21. Boissard F, Fournié JJ, Laurent C, Poupot M, Ysebaert L. Nurse like cells: chronic lymphocytic leukemia associated macrophages. *Leuk Lymphoma.* 2015;56(5):1570-1572.

22. Lai C, Stepniak D, Sias L, Funatake C. A sensitive flow cytometric method for multi-parametric analysis of microRNA, messenger RNA and protein in single cells. *Methods.* 2018;134-135:136-148.

23. Panse J, Friedrichs K, Marx A, et al. Chemokine CXCL13 is overexpressed in the tumour tissue and in the peripheral blood of breast cancer patients. *Br J Cancer.* 2008;99(6):930-938.

24. Weber M, Hauschild R, Schwarz J, et al. Interstitial dendritic cell guidance by haptotactic chemokine gradients. *Science.* 2013;339(6117):328-332.

25. Niemann CU, Herman SE, Maric I, et al. Disruption of in vivo chronic lymphocytic leukemia tumor-microenvironment interactions by ibrutinib: findings from an investigator-initiated phase II study. *Clin Cancer Res.* 2016;22(7):1572-1582.

26. Fiorcari S, Maffei R, Audrito V, et al. Ibrutinib modifies the function of monocyte/macrophage population in chronic lymphocytic leukemia. *Oncotarget.* 2016;7(40):65968-65981.

27. Boissard F, Fournié JJ, Quillet-Mary A, Ysebaert L, Poupot M. Nurse-like cells mediate ibrutinib resistance in chronic lymphocytic leukemia patients. *Blood Cancer J.* 2015;5(10):e355.

28. Victora GD, Schwickert TA, Fooksman DR, et al. Germinal center dynamics revealed by multiphoton microscopy with a photoactivatable fluorescent reporter. *Cell.* 2010;143(4):592-605.

29. López-Giral S, Quintana NE, Cabrerizo M, et al. Chemokine receptors that mediate B cell homing to secondary lymphoid tissues are highly expressed in B cell chronic lymphocytic leukemia and non-Hodgkin lymphomas with widespread nodular dissemination. *J Leukoc Biol.* 2004;76(2):462-471.

30. Burger JA, Li KW, Keating MJ, et al. Leukemia cell proliferation and death in chronic lymphocytic leukemia patients on therapy with the BTK inhibitor ibrutinib. *JCI Insight.* 2017;2(2):e89904.

31. Luther SA, Tang HL, Hyman PL, Farr AG, Cyster JG. Coexpression of the chemokines ELC and SLC by T zone stromal cells and deletion of the ELC gene in the plt/plt mouse. *Proc Natl Acad Sci USA.* 2000;97(23):12694-12699.

32. Batista FD, Arana E, Barral P, et al. The role of integrins and coreceptors in refining thresholds for B-cell responses. *Immunol Rev.* 2007;218(1): 197-213.

33. Link A, Vogt TK, Favre S, et al. Fibroblastic reticular cells in lymph nodes regulate the homeostasis of naive T cells. *Nat Immunol.* 2007;8(11): 1255-1265.

34. Schumann K, Lämmermann T, Bruckner M, et al. Immobilized chemokine fields and soluble chemokine gradients cooperatively shape migration patterns of dendritic cells. *Immunity.* 2010;32(5):703-713.

35. Hirose J, Kawashima H, Swope Willis M, et al. Chondroitin sulfate B exerts its inhibitory effect on secondary lymphoid tissue chemokine (SLC) by binding to the C-terminus of SLC. *Biochim Biophys Acta.* 2002;1571(3):219-224.

36. Boissard F, Tosolini M, Ligat L, et al. Nurse-like cells promote CLL survival through LFA-3/CD2 interactions. *Oncotarget.* 2016;8(32):52225-52236.

37. Domagala M, Ysebaert L, Ligat L, et al. IL-10 rescues CLL survival through repolarization of inflammatory nurse-like cells. *Cancers (Basel).* 2021; 14(1):16.

38. Boissard F, Laurent C, Ramsay AG, et al. Nurse-like cells impact on disease progression in chronic lymphocytic leukemia. *Blood Cancer J.* 2016; 6(1):e381.

39. Wang Y, Sinha S, Wellik LE, et al. Distinct immune signatures in chronic lymphocytic leukemia and Richter syndrome. *Blood Cancer J.* 2021; 11(5):86.